



HAL
open science

Rare gas systematics on Lucky Strike basalts (37°N, North Atlantic): Evidence for efficient homogenization in a long-lived magma chamber system?

Manuel Moreira, Javier Escartin, Eric Gayer, Cédric Hamelin, Antoine Bézos, Fabien Guillon, Mathilde Cannat

► To cite this version:

Manuel Moreira, Javier Escartin, Eric Gayer, Cédric Hamelin, Antoine Bézos, et al.. Rare gas systematics on Lucky Strike basalts (37°N, North Atlantic): Evidence for efficient homogenization in a long-lived magma chamber system?. *Geophysical Research Letters*, 2011, 38 (8), pp.L08304. 10.1029/2011GL046794 . hal-02330261

HAL Id: hal-02330261

<https://hal.science/hal-02330261>

Submitted on 23 Oct 2019

HAL is a multi-disciplinary open access archive for the deposit and dissemination of scientific research documents, whether they are published or not. The documents may come from teaching and research institutions in France or abroad, or from public or private research centers.

L'archive ouverte pluridisciplinaire **HAL**, est destinée au dépôt et à la diffusion de documents scientifiques de niveau recherche, publiés ou non, émanant des établissements d'enseignement et de recherche français ou étrangers, des laboratoires publics ou privés.

Rare gas systematics on Lucky Strike basalts (37°N, North Atlantic): Evidence for efficient homogenization in a long-lived magma chamber system?

Manuel Moreira,¹ Javier Escartin,¹ Eric Gayer,¹ Cédric Hamelin,¹ Antoine Bezos,² Fabien Guillon,¹ and Mathilde Cannat¹

Received 15 January 2011; revised 3 March 2011; accepted 8 March 2011; published 20 April 2011.

[1] We present rare gas data in fresh glasses from the Lucky Strike segment located on the Mid Atlantic Ridge (~37.3°N), close to the Azores plateau. We analyzed the helium and neon isotopes in 28 samples by melting as well as He-Ne-Ar-Kr-Xe isotopes in 9 samples by crushing. Samples were collected during the Graviduck06, MOMAR08, and Bathyluck09 cruises over a ridge length of ~13 km (mean sample spacing of ~500 m), and at depths ranging from 1550 m to 2174 m. The helium isotopic ratio varies between 84,410 and 88,235 (R/Ra between 8.19 and 8.56). The samples having the “most” primitive helium isotopic ratio are the enriched samples (e.g. high K₂O/TiO₂) although the difference to the depleted samples is small. It appears that all of our samples derive from the same and well-homogenized magma chamber. Neon isotopes clearly show the influence of the Azores hotspot, which is not seen with helium because of lower ³He/²²Ne in the plume source compared to the MORB source. **Citation:** Moreira, M., J. Escartin, E. Gayer, C. Hamelin, A. Bezos, F. Guillon, and M. Cannat (2011), Rare gas systematics on Lucky Strike basalts (37°N, North Atlantic): Evidence for efficient homogenization in a long-lived magma chamber system?, *Geophys. Res. Lett.*, 38, L08304, doi:10.1029/2011GL046794.

1. Introduction

[2] Rare gases are excellent tracers of plume-ridge interaction due to the primitive signature seen in Oceanic island basalts (OIB). Indeed, Mid Oceanic Ridge Basalts (MORB) show a ⁴He/³He ratio of 90,000 ± 10,000 (R/Ra = 8 ± 1 where R is the ³He/⁴He ratio and Ra is the atmospheric ratio of 1.384 · 10⁻⁶) whereas OIB show lower ratios (higher R/Ra), down to 15,000 (R/Ra = 50) for the ancient Iceland plume [Stuart *et al.*, 2003]. To explain the lower ⁴He/³He ratios in OIB than in MORB, it is generally proposed that mantle plumes sample a gas-rich reservoir [Kurz *et al.*, 1982]. Neon isotopes show a similar behavior to that of helium isotopes. The ²¹Ne/²²Ne ratio is lower in OIB than in MORB [Honda *et al.*, 1991; Valbracht *et al.*, 1997]. Because the ²¹Ne is nucleogenic (e.g. ¹⁸O(α,n)²¹Ne or ²⁴Mg(n,α)²¹Ne),

it is generally proposed that in order to preserve a lower ²¹Ne/²²Ne, the OIB source has to be enriched in ²²Ne compared to the MORB source. Therefore, both helium and neon are very sensitive to plume-derived magmas due to these expected high concentrations. Previous studies have demonstrated the interest of measuring the rare gases to constrain plume-ridge interactions [Graham *et al.*, 1999; Hopp *et al.*, 2004; Moreira *et al.*, 1995; Poreda *et al.*, 1986; Sarda *et al.*, 2000; Stroncik *et al.*, 2008].

[3] The objective of this study is to constrain the influence of the Azores hotspot along the Mid Atlantic Ridge, as well as to investigate the scale of mantle heterogeneities. We present helium and neon isotopes in 28 samples from the Lucky Strike segment, North Atlantic (37°20'N), as well as He-Ne-Ar-Kr-Xe elemental compositions and isotopic ratios in 9 samples from this segment.

2. Lucky Strike Segment and Sampling

[4] The ~70 km-long Lucky strike segment is centered at ~37°20'N on the Mid Atlantic Ridge, and ~350 km West of the Azores hotspot. It shows a 15–20 km wide axial valley with axial depths that vary from >4000 m at the segment ends to 1550 m at the center of the segment. The volcano located at the center of the segment is ~10 km wide and 15 km long along the ridge axis, and hosts an active hydrothermal field discovered in 1992 during the FAZAR cruise [Langmuir *et al.*, 1997]. A depression at the summit of the volcano, surrounded by three highs, hosts the hydrothermal fields and a lava lake (Figure 1). An axial magma chamber (AMC) is present at a depth of 3.4 km below the seafloor under the volcano, and extends ~7 km along axis and ~3 km perpendicular to it [Singh *et al.*, 2006]. This AMC probably supplies the heat necessary for the hydrothermal field and may be the source of the erupted lava flows. From a geochemical point of view, basalts from the Lucky Strike segment are enriched in incompatible elements [Langmuir *et al.*, 1997]. Samples were collected during the Graviduck06, MOMAR08 and Bathyluck09 cruises over a distance of ~13 km (mean sample spacing of ~500 m). Sampling depths vary from 1550 m to 2174 m. Note that we have duplicated a previously analyzed sample from the FAZAR cruise, A127 D15-1 [Moreira and Allègre, 2002] and provided by C. Langmuir. All the analyses are from glass samples, except for two olivines picked from picritic basalts (GRA N16-8 and GRA N17-4) without glass. Two samples (GRARC07 and MOM08V02) are considered as very enriched in trace elements (e.g. high K/Ti

¹Institut de Physique du Globe de Paris, Sorbonne Paris Cité CNRS, UMR 7154, Paris, France.

²Laboratoire de Planetologie et de Géodynamique de Nantes, Faculté des Sciences, Nantes, France.

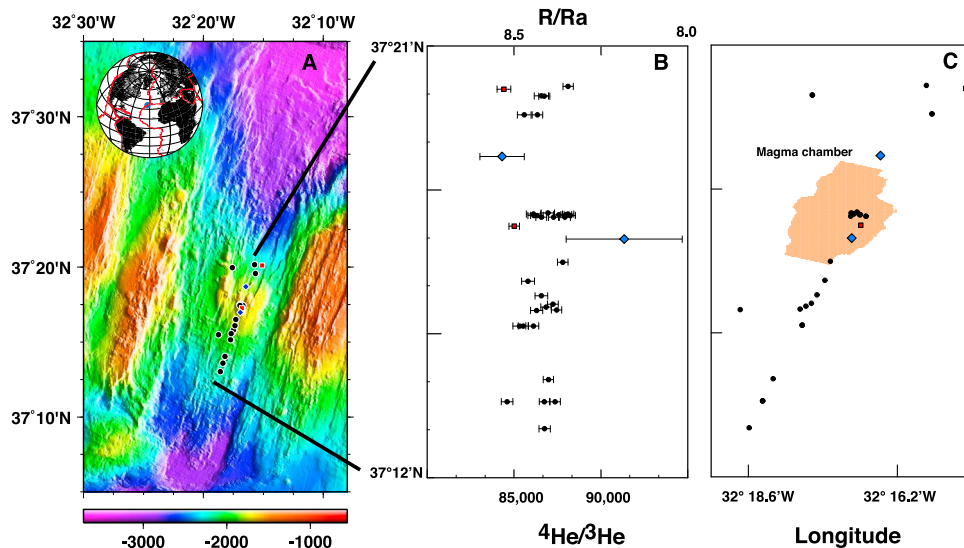


Figure 1. (a) Bathymetric map of the Lucky Strike segment with sample locations. Black dots are N-MORB samples, blue diamonds are picrites (no glass), and red squares are E-MORB according to their higher K/Ti ratio. The insert gives the location of the Lucky Strike segment (LS). Bathymetric data from *Cannat et al.* [1999], *Escartin et al.* [2001], *Fouquet and Party* [1997]. (b) Helium isotopic ratios in Lucky Strike samples reported against latitude. (c) Sample location and projection at the surface of the magma chamber located 3 km beneath the sea floor [*Combiér, 2007*].

ratio) compared to the other samples (A. Bezou, unpublished data, 2011).

3. Analytical Procedure and Results

[5] Samples were cleaned with distilled water and ethanol in an ultrasonic bath. When Mn crust was present, peroxide was used. Two noble gas mass spectrometers were used for this study: ARESIBO II and our new Noblesse (Nu instruments ©). Crushing and melting under vacuum was used for the gas extraction. Only He and Neon were analyzed on the Noblesse whereas the abundances of the five rare gases were determined, as well as isotopic ratios of He-Ne and Ar, on the ARESIBO II mass spectrometer. The analytical procedure on ARESIBO II is given by *Moreira and Allègre* [2002]. The Noblesse mass spectrometer analytical procedure will be given elsewhere. During the course of the Lucky Strike segment analyses, the precision (1 standard deviation) of the standards was 0.3% for the helium isotopic ratios and 0.2% and 0.5% for $^{20}\text{Ne}/^{22}\text{Ne}$ and $^{21}\text{Ne}/^{22}\text{Ne}$, respectively.

[6] Blanks were $1.4 \cdot 10^{-10}$ ccSTP for ^4He and $7 \cdot 10^{-14}$ ccSTP for ^{22}Ne for the crushing experiments whereas they were $1.4 \cdot 10^{-10}$ ccSTP for ^4He and between $8 \cdot 10^{-13}$ and $3 \cdot 10^{-12}$ ccSTP for ^{22}Ne for the melting procedure. A single heating step at 1400°C was applied on the samples.

[7] Rare gas results are given in Tables 1 and 2. Bulk helium concentrations in glass samples vary from $3 \cdot 10^{-6}$ to $2.2 \cdot 10^{-5}$ ccSTP/g, typical of MORB, whereas crushing experiments give slightly lower helium concentration ($3 \cdot 10^{-6}$ to $8.5 \cdot 10^{-6}$ ccSTP/g). Olivine samples give concentration of $5.2 \cdot 10^{-9}$ and $1.1 \cdot 10^{-8}$ ccSTP/g, typical of concentrations in olivines. The $^4\text{He}/^3\text{He}$ ratio varies from 84,409 to 88,235 for the melted glass samples. Crushed glasses give lower helium isotopic ratios, from $78,540 \pm 1540$ to $87,790 \pm 18,30$. The two olivine samples gave $^4\text{He}/^3\text{He}$ ratios of $91,350 \pm 3350$ and $84,310 \pm 1280$. All the isotopic ratios are typical of

MORB. The two most incompatible element enriched samples (GRARC07 and MOM08V02) do not present helium isotopic ratios different from the depleted samples: 84,409 and 85,005, respectively (Figure 1b).

[8] ^{22}Ne concentrations vary from $2.3 \cdot 10^{-12}$ to $4.8 \cdot 10^{-10}$ ccSTP/g for melted samples and from $1.54 \cdot 10^{-12}$ to $1.42 \cdot 10^{-11}$ ccSTP/g for crushing. $^{20}\text{Ne}/^{22}\text{Ne}$ ratios vary from 9.97 to 12.09 for melting experiments and from 10.42 to 12.29 for the crushing ones. The $^{21}\text{Ne}/^{22}\text{Ne}$ is correlated with $^{20}\text{Ne}/^{22}\text{Ne}$ and varies from 0.0300 to 0.0499 (melting) and from 0.0335 to 0.0481 (crushing). Results are plotted on Figure 2. Samples from Lucky Strike fall on a different line than the classical MORB line defined by [*Sarda et al., 1988*]. Note that both mass spectrometers give the same neon systematics.

[9] ^{36}Ar concentrations vary from $1.1 \cdot 10^{-11}$ to $3.2 \cdot 10^{-10}$ ccSTP/g (only crushing) and is correlated to ^{22}Ne abundances (not shown). $^{38}\text{Ar}/^{36}\text{Ar}$ ratios are between 0.1878 and 0.1911 (air = 0.1880). $^{40}\text{Ar}/^{36}\text{Ar}$ ratios are between 482 and 3439. The highest ratio (3439) is far from the mantle value estimated at $\sim 30,000$ [*Staudacher et al., 1989*]. ^{84}Kr and ^{130}Xe abundances are correlated with neon and argon abundances. ^{84}Kr is comprised between $3.2 \cdot 10^{-13}$ and $9.6 \cdot 10^{-12}$ ccSTP/g. ^{130}Xe varies from $2.1 \cdot 10^{-15}$ and $5.7 \cdot 10^{-14}$ ccSTP/g. Heavy rare gases will not be discussed in this paper. Indeed, $^{40}\text{Ar}/^{36}\text{Ar}$ ratios correlate with the $^{20}\text{Ne}/^{22}\text{Ne}$ (not shown). This correlation can be interpreted as the result of a mixture between a magmatic component and an atmospheric component. The $[\text{Ne}/^{36}\text{Ar}]_{\text{Magmatic}}/[\text{Ne}/^{36}\text{Ar}]_{\text{air}}$ that is necessary to explain the Ne-Ar correlation is ~ 50 , far above the ratio observed for undegassed samples such as the popping rock 2 π D43, which presents a ratio of 1.6 [*Moreira et al., 1998*]. Such a strong hyperbolic mixture doesn't allow the determination of the uncontaminated $^{40}\text{Ar}/^{36}\text{Ar}$ ratio of the Lucky Strike magma. This high $[\text{Ne}/^{36}\text{Ar}]_{\text{Magmatic}}/[\text{Ne}/^{36}\text{Ar}]_{\text{air}}$ ratio clearly reflects the

Table 1. He and Ne Results Obtained by Melting at 1400°C and Crushing on the Noblesse Mass Spectrometer. Concentrations are in CCSTP/g. Uncertainties on Concentrations are 5%. Dup Means Duplicate.

Samples	Lat (°N)	Long (°E)	Depth (m)	Weight (g)	⁴ He (×10 ⁻⁶)	⁴ He/ ³ He	σ	R/Ra	σ	²² Ne	²⁰ Ne/ ²² Ne	σ	²¹ Ne/ ²² Ne	σ
GRA-N2-2	37.3261	-32.2607	2080	0.027	4.03	85587	396	8.44	0.04					
GRA-N2-2 dup	37.3261	-32.2607	2080	0.049	5.45	86346	310	8.37	0.03	1.08 10 ⁻¹¹	10.41	0.15	0.0391	0.0017
GRA-N3-1	37.3326	-32.2928	1951	0.046	4.49	86740	312	8.33	0.03					
GRA-N3-2	37.3327	-32.2929	1946	0.035	4.78	86573	415	8.35	0.04	4.06 10 ⁻¹¹	10.03	0.06	0.0313	0.0010
GRA-N4-1	37.2920	-32.2808	1743	0.096	10.5	86947	387	8.31	0.04	6.08 10 ⁻¹²	12.07	0.25	0.0485	0.0026
GRA-N7-1	37.2916	-32.2824	1735	0.075	8.37	86120	418	8.39	0.04	1.15 10 ⁻¹¹	10.96	0.11	0.0388	0.0015
GRA-N7-1 dup	37.2916	-32.2824	1735	0.083	8.41	88115	322	8.20	0.03					
GRA-N16-1	37.2581	-32.3122	2027	0.050	3.07	86303	353	8.37	0.03	9.50 10 ⁻¹¹	10.02	0.03	0.0300	0.0003
GRA-N16-2	37.2583	-32.2961	1916	0.074	8.76	87449	293	8.26	0.03	4.98 10 ⁻¹¹	10.18	0.03	0.0316	0.0003
GRA-N16-3	37.2603	-32.2931	1895	0.053	7.04	87235	312	8.28	0.03					
GRA-N16-4	37.2632	-32.2916	1847	0.093	9.71	86575	360	8.35	0.03	8.48 10 ⁻¹¹	10.06	0.03	0.0306	0.0002
GRA-N16-5	37.2683	-32.2895	1803	0.067	9.30	85805	378	8.42	0.04	1.22 10 ⁻¹¹	11.11	0.11	0.0393	0.0012
GRA-N16-6	37.2749	-32.2880	1770	0.056	8.58	87800	301	8.23	0.03	1.77 10 ⁻¹¹	10.37	0.06	0.0347	0.0007
GRA-N17-1	37.3360	-32.2622	2128	0.277	6.14	88115	299	8.20	0.03	2.01 10 ⁻¹¹	10.41	0.04	0.0325	0.0003
GRA-N22-1	37.2170	-32.3098	2174	0.027	7.94	86759	329	8.33	0.03					
GRA-N22-2	37.2264	-32.3062	2147	0.130	9.19	84600	332	8.54	0.03	9.04 10 ⁻¹¹	10.15	0.03	0.0304	0.0002
GRA-N22-2 dup	37.2264	-32.3062	2147	0.201	7.39	86747	293	8.33	0.03	2.22 10 ⁻¹¹	10.33	0.06	0.0332	0.0006
GRA-N22-2 dup	37.2264	-32.3062	2147	0.072	8.20	87369	299	8.27	0.03	1.86 10 ⁻¹¹	10.35	0.04	0.0332	0.0004
GRA-N22-3	37.2341	-32.3034	2118	0.071	7.39	86977	298	8.31	0.03	6.08 10 ⁻¹²	11.37	0.18	0.0395	0.0019
GRA-N22-5	37.2527	-32.2956	1833	0.141	5.02	85306	369	8.47	0.04	4.81 10 ⁻¹⁰				
GRA-N22-5 dup	37.2527	-32.2956	1833	0.079	7.08	85524	288	8.45	0.03	1.24 10 ⁻¹⁰	10.05	0.03	0.0303	0.0003
GRA-N22-5 dup	37.2527	-32.2956	1833	0.081	7.08	86120	294	8.39	0.03	2.33 10 ⁻¹¹	10.63	0.06	0.0339	0.0005
GRA-N22-6	37.2593	-32.2946	1887	0.163	9.70	86844	297	8.32	0.03	2.09 10 ⁻¹¹	10.49	0.04	0.0345	0.0005
B09 ROC07	37.2914	-32.2817		0.185	9.56	87580	301	8.25	0.03	2.79 10 ⁻¹¹	10.31	0.03	0.0332	0.0003
B09 ROC08	37.2914	-32.2817		0.055	6.42	88008	315	8.21	0.03	2.33 10 ⁻¹²				
B09 ROC20	37.2911	-32.2802		0.200	11.7	86149	357	8.39	0.03	4.64 10 ⁻¹¹	10.33	0.03	0.0324	0.0003
B09 ROC21	37.2911	-32.2800		0.073	9.98	86320	364	8.37	0.04	2.28 10 ⁻¹¹	10.48	0.04	0.0347	0.0006
B09 ROC22	37.2911	-32.2800		0.067	8.69	88235	299	8.19	0.03	5.53 10 ⁻¹²	12.09	0.36	0.0499	0.0040
B09 ROC23	37.2905	-32.2784		0.047	7.08	86566	313	8.35	0.03					
B09 ROC24	37.2905	-32.2784		0.090	8.02	87275	288	8.28	0.03	2.48 10 ⁻¹¹	10.48	0.05	0.0330	0.0005
A127 D15-1	37.2905	-32.2825	1706		10.4	87927	319	8.22	0.03	1.50 10 ⁻¹⁰	9.97	0.03	0.0301	0.0003
GRA RC07	37.3350	-32.2516	2160	0.051	2.05	84409	394	8.56	0.04	7.00 10 ⁻¹²	11.78	0.13	0.0491	0.0021
MOM08V02	37.2874	-32.2798	1629	0.022	21.7	85005	300	8.50	0.03	4.33 10 ⁻¹⁰	10.34	0.03	0.0326	0.0003
CRUSHING OLIVINES														
GRA-N16-8 (olivines)	37.2829	-32.2822	1550	0.205	5.18 10 ⁻⁹	91346	3349	7.91	0.29					
GRA-N17-4 (olivines)	37.3116	-32.2745	1779	0.474	1.14 10 ⁻⁸	84311	1279	8.57	0.13	7.60 10 ⁻¹³	9.91	0.08	0.0296	0.0006

high degassing rate of the samples as illustrated by the high ⁴He/⁴⁰Ar* ratios (Table 2).

4. Discussion

4.1. Homogeneity of the Helium Isotopic Ratios and the Evidence for a Well-Mixed Magma Chamber

[10] Figure 1b shows the helium isotopic ratio obtained by melting reported versus the latitude. Ratios show very homogeneous results, with a mean ratio of $86,649 \pm 1010$ (R/Ra = 8.34 ± 0.09). Olivine samples from two picrites give the same helium isotopic ratio as the glass samples within uncertainties. The isotopic variation (~1%) is small compared to that reported for a complete ridge (few percents) [Allègre *et al.*, 1995] or a ridge section (~3% for SWIR [Georgen *et al.*, 2003]).

[11] At that point, it is clear that we are not able to distinguish with helium any peculiar chemical heterogeneity in the mantle source of Lucky Strike segment. If the mantle has a marble cake structure [Allègre and Turcotte, 1986], the enriched component (e.g. pyroxenite) is easily homogenized with the depleted one for helium at the scale of our sampling interval (13 km along-axis). Homogenization could occur

before melting by diffusion of helium in the mantle [Hart *et al.*, 2008], homogenization by small-scale convection in the uppermost upper mantle [Graham *et al.*, 2001] or, more probably, after melting in a magma chamber considering the scale of our study. In this last case, we could conclude that all the MORBs from the Lucky Strike segment sample the same magma chamber, which was seismically imaged [Singh *et al.*, 2006].

4.2. Evidence for the Azores Influence on the Lucky Strike Volcano Source

[12] Azores island basalts are characterized by both relatively low ⁴He/³He ratios (high R/Ra) for the islands from the central group and by radiogenic helium for São Miguel island [Moreira *et al.*, 1999]. The interpretation for these helium isotopic ratios is the presence of a mantle plume deriving from a primitive mantle and centered under the central group, in agreement with melt fluxes [Bourdon *et al.*, 2005] and seismology [Yang *et al.*, 2006], and with the presence of a chemical heterogeneity with crustal affinity under São Miguel island [Beier *et al.*, 2008]. Neon systematics also suggest a primitive signature for the Azores hotspot [Madureira *et al.*, 2005].

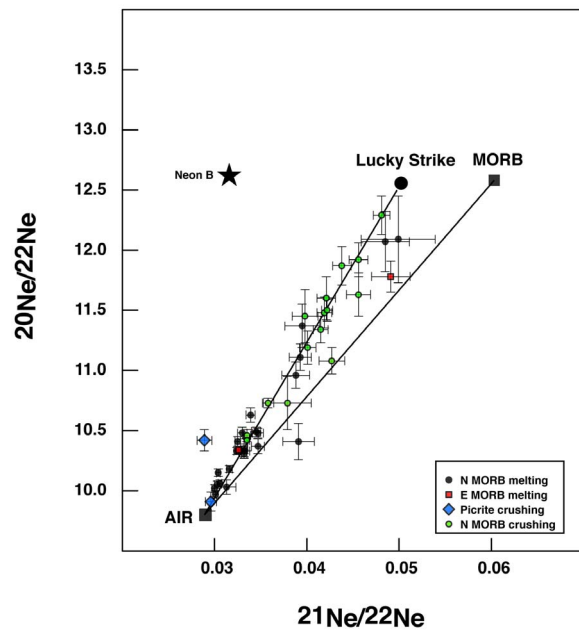


Figure 2. Three-isotope neon diagram. The MORB composition is derived from *Sarda et al.* [1988]. MORB from the Lucky strike segment show a different slope in this diagram, which can be attributed to mixing with a component having primitive neon. Uncertainties are 1σ .

[13] The helium isotopic ratios of samples from Lucky Strike are not different from the normal MORB value. Indeed, the mean north Atlantic MORB ratio is $89,380 \pm 9300$ [*Allègre et al.*, 1995] whereas the mean helium ratio of Lucky Strike samples is $86,480 \pm 1180$. Therefore, based

only on the helium isotopes, the Azores hotspot influence cannot be seen in the Lucky Strike segment.

[14] Neon isotopes give a different view of the Azores influence from that of helium. Indeed, as illustrated by Figure 2, the slope of the Lucky Strike samples in the three-isotope neon diagram is higher than the MORB line defined by [*Sarda et al.*, 1988]. This line is interpreted as reflecting a mixing between a mantle-derived component and an atmosphere-derived component (e.g. crust assimilation, seawater interaction, air introduction in the samples). That different slope than MORB means that the mantle beneath Lucky strike has a lower $^{21}\text{Ne}/^{22}\text{Ne}$ than the normal Atlantic mantle and this can be attributed to the Azores hotspot influence. Figure 3 shows the $^4\text{He}/^3\text{He}$ versus the $^{21}\text{Ne}/^{22}\text{Ne}$ isotopic ratio extrapolated to $^{20}\text{Ne}/^{22}\text{Ne} = 12.6$ (e.g. corrected for air contamination), which corresponds to the value of the “Neon B”, representative of the mantle value [*Raquin and Moreira, 2009; Trieloff et al.*, 2000]. Mantle plume magmas have lower $^3\text{He}/^{22}\text{Ne}$ ratio than the MORB magmas (by a factor 5 to 10) [*Moreira et al.*, 2001; *Yokochi and Marty, 2004*] due either to different $^3\text{He}/^{22}\text{Ne}$ ratios in the two sources, or to mixing of degassed magmas [e.g., *Moreira et al.*, 2001]. Therefore, in Figure 3, mixing is not linear but hyperbolic, which means that neon is more sensitive to the Azores mantle source influence than helium. The isotopic ratios for Terceira Island (Azores) and Lucky strike segment are reported on Figure 3. One can clearly see that the Lucky Strike magma are a mixture between magma from the normal MORB mantle and magma from a primitive component, being the Azores mantle plume.

5. Conclusions

[15] Rare gases in MORB from the central part of the Lucky Strike segment show that the mantle beneath this

Table 2. Rare Gas Results Obtained by Crushing on the ARESIBOII Mass Spectrometer^a

Sample	Lat (°N)	Long (°E)	Depth (m)		^4He ($\times 10^{-6}$)	^{22}Ne ($\times 10^{-12}$)	^{36}Ar	^{84}Kr	^{130}Xe	$^4\text{He}/^{40}\text{Ar}^*$	σ															
GRA-N2-2	37.3261	-32.2607	2080		3.06	6.00	$1.18 \cdot 10^{-10}$	$4.15 \cdot 10^{-12}$	$3.58 \cdot 10^{-14}$	24	1															
GRA-N4-1	37.2920	-32.2808	1743	step1	2.91	3.67	$4.42 \cdot 10^{-11}$	$1.22 \cdot 10^{-12}$	$7.02 \cdot 10^{-15}$	74	4															
				step2	1.37	1.54	$1.14 \cdot 10^{-11}$	$3.23 \cdot 10^{-13}$	$2.12 \cdot 10^{-15}$	62	3															
				Total	4.28	5.21	$5.56 \cdot 10^{-11}$	$1.55 \cdot 10^{-12}$	$9.14 \cdot 10^{-15}$	70	4															
					3.63	5.38	$1.15 \cdot 10^{-10}$	$3.84 \cdot 10^{-12}$	$2.00 \cdot 10^{-14}$	58	3															
GRA-N7-1	37.2916	-32.2824	1735		3.63	5.38	$1.15 \cdot 10^{-10}$	$3.84 \cdot 10^{-12}$	$2.00 \cdot 10^{-14}$	58	3															
GRA-N16-3	37.2604	-32.2932	1895		3.52	4.24	$3.73 \cdot 10^{-11}$	$1.08 \cdot 10^{-12}$	$6.05 \cdot 10^{-15}$	66	3															
GRA-N16-6	37.2749	-32.2880	1770		3.20	14.2	$3.16 \cdot 10^{-10}$	$9.62 \cdot 10^{-12}$	$5.67 \cdot 10^{-14}$	54	3															
GRA-N22-2	37.2264	-32.3062	2147		3.16	3.44	$2.97 \cdot 10^{-11}$	$8.99 \cdot 10^{-13}$	$5.35 \cdot 10^{-15}$	191	10															
GRA-N22-3	37.2341	-32.3034	2118		3.77	3.66	$2.95 \cdot 10^{-11}$	$1.06 \cdot 10^{-12}$	$5.46 \cdot 10^{-15}$	200	11															
B09 ROC20	37.2912	-32.2802			5.25	4.47	$2.85 \cdot 10^{-11}$	$8.96 \cdot 10^{-13}$	$5.26 \cdot 10^{-15}$	76	4															
B09 ROC21	37.2905	-32.2800			4.81	4.00	$2.09 \cdot 10^{-11}$	$6.35 \cdot 10^{-13}$	$5.32 \cdot 10^{-15}$	73	4															
Sample					$^4\text{He}/^3\text{He}$	σ	R/Ra	σ	$^{20}\text{Ne}/^{22}\text{Ne}$	σ	$^{21}\text{Ne}/^{22}\text{Ne}$	σ	$^{38}\text{Ar}/^{36}\text{Ar}$	σ	$^{40}\text{Ar}/^{36}\text{Ar}$	σ										
GRA-N2-2					82060	1617	8.81	0.17	11.48	0.13	0.0419	0.0008	0.1888	0.0004	1356	8										
GRA-N4-1	step1	83457	1924	8.66	0.20	11.34	0.11	0.0415	0.0008	0.1884	0.0003	1182	7													
														step2	87386	1713	8.27	0.16	11.87	0.16	0.0438	0.0010	0.1894	0.0004	2236	18
															87794	1832	8.23	0.17	11.19	0.14	0.0401	0.0009	0.1902	0.0003	840	5
GRA-N7-1					81094	1638	8.91	0.18	11.63	0.18	0.0456	0.0013	0.1900	0.0005	1733	14										
GRA-N16-3					84017	1661	8.60	0.17	10.42	0.09	0.0335	0.0003	0.1878	0.0003	482	3										
GRA-N16-6					78537	1537	9.20	0.18	11.60	0.18	0.0421	0.0010	0.1889	0.0005	854	6										
GRA-N22-2					83531	1809	8.65	0.19	11.45	0.22	0.0398	0.0014	0.1902	0.0006	935	12										
B09 ROC20					85005	1733	8.50	0.17	11.92	0.14	0.0456	0.0010	0.1900	0.0005	2733	19										
B09 ROC21					87264	1840	8.28	0.17	12.29	0.16	0.0481	0.0009	0.1911	0.0005	3439	31										

^aConcentrations are in CCSTP/g. Uncertainties on concentrations are 5%.

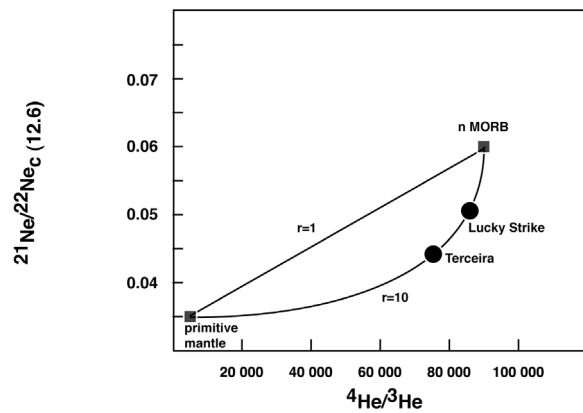


Figure 3. Extrapolated $^{21}\text{Ne}/^{22}\text{Ne}$ ratios of the regression line of all Lucky Strike samples (at a $^{20}\text{Ne}/^{22}\text{Ne}$ of 12.6) plotted versus the mean $^4\text{He}/^3\text{He}$ ratio. The hyperbola is derived from [Kurz et al., 2009]. The Terceira Island (Azores) isotopic ratios are given by Madureira et al. [2005]. The r parameter is $^3\text{He}/^{22}\text{Ne}_{\text{MORB}}/^3\text{He}/^{22}\text{Ne}_{\text{Primitive mantle}}$. For most OIB and on-ridge hotspots, r is close to 10 [Kurz et al., 2009; Moreira and Allègre, 1998].

segment is extremely homogeneous. Neon isotopes clearly suggest the influence of the Azores hotspot, although this is not seen with helium isotopes. We conclude that all the analyzed samples derive from the same central magma chamber, and that it is very well homogenized. This is easily achieved for helium, and may be neon, due to their high diffusivity in melt.

[16] **Acknowledgments.** We acknowledge the effort and support of the officers, crew, and science parties of the Graveluck'06, MoMAR'08, and Bathyluck'09 cruises and the team operating the Nautilie submersible and the VICTOR remotely operated vehicle. Ship time was financed by CNRS/INSU and IFREMER, with additional support from ANR (MOTHSEIM Project NT05-3_42213) to J. Escartin. Philippe Sarda and Pete Burnard are thanked for their very constructive reviews. The editor thanks Pete Burnard and Philippe Sarda for their review.

References

Allègre, C. J., and D. Turcotte (1986), Implications of a two-component marble-cake mantle, *Nature*, *323*, 123–127, doi:10.1038/323123a0.

Allègre, C. J., M. Moreira, and T. Staudacher (1995), $^4\text{He}/^3\text{He}$ dispersion and mantle convection, *Geophys. Res. Lett.*, *22*(17), 2325–2328, doi:10.1029/95GL02307.

Beier, C., K. Haase, W. Abouchami, M.-S. Krienitz, and F. Hauff (2008), Magma genesis by rifting of oceanic lithosphere above anomalous mantle: Terceira Rift, Azores, *Geochem. Geophys. Geosyst.*, *9*, Q12013, doi:10.1029/2008GC002112.

Bourdon, B., S. P. Turner, and N. M. Ribe (2005), Partial melting and upwelling rates beneath the Azores from a U-series isotope perspective, *Earth Planet. Sci. Lett.*, *239*, 42–56, doi:10.1016/j.epsl.2005.08.008.

Cannat, M., et al. (1999), Mid-Atlantic ridge - Azores hotspot interactions: Along-axis migration of a hotspot-derived magmatic pulse 14 to 4 Myrs ago, *Earth Planet. Sci. Lett.*, *173*, 257–269, doi:10.1016/S0012-821X(99)00234-4.

Combier, V. (2007), Mid-Ocean Ridge processes: Insights from 3D refraction seismics at the 9°N OSC on the East Pacific Rise, and the Lucky Strike volcano on the Mid-Atlantic Ridge, Ph.D. thesis, Inst. de Phys. du Globe de Paris, Paris.

Escartin, J., M. Cannat, G. Poulouquen, A. Rabain, and J. Lin (2001), Crustal thickness of V-shaped ridges south of the Azores: Interaction of the Mid-Atlantic Ridge (36° – 39°N) and the Azores hot spot, *J. Geophys. Res.*, *106*, 21,719–21,735, doi:10.1029/2001JB000224.

Fouquet, Y., and S. Party (1997), FLORES cruise, AMORES project of the European MAST III programme, Plouzané, IFREMER, Cruise report.

Georgen, J. E., M. Kurz, H. J. B. Dick, and J. Lin (2003), Low $^3\text{He}/^4\text{He}$ ratios in basalt glasses from the western southwest Indian Ridge (10 – 24°E), *Earth Planet. Sci. Lett.*, *206*, 509–528, doi:10.1016/S0012-821X(02)01106-8.

Graham, D. W., K. T. M. Johnson, L. Douglas Priebe, and J. E. Lupton (1999), Hotspot-ridge interaction along the southeast Indian Ridge near Amsterdam and St Paul islands: Helium isotope evidence, *Earth Planet. Sci. Lett.*, *167*, 297–310, doi:10.1016/S0012-821X(99)00030-8.

Graham, D. W., J. E. Lupton, F. J. Spera, and D. M. Christie (2001), Upper-mantle dynamics revealed by helium isotope variations along the southeast Indian Ridge, *Nature*, *409*, 701–703, doi:10.1038/35055529.

Hart, S., M. D. Kurz, and Z. Wang (2008), Scale length of mantle heterogeneities: Constraints from helium diffusion, *Earth Planet. Sci. Lett.*, *269*, 508–517, doi:10.1016/j.epsl.2008.03.010.

Honda, M., I. McDougall, D. B. Patterson, A. Doulgeris, and D. Clague (1991), Possible solar noble-gas component in Hawaiian basalts, *Nature*, *349*, 149–151, doi:10.1038/349149a0.

Hopp, J., M. Tieloff, and R. Altherr (2004), Neon isotopes in mantle rocks from the Red Sea region reveal large-scale plume-lithosphere interaction, *Earth Planet. Sci. Lett.*, *219*, 61–76, doi:10.1016/S0012-821X(03)00691-5.

Kurz, M. D., W. J. Jenkins, and S. R. Hart (1982), Helium isotopic systematics of oceanic islands and mantle heterogeneity, *Nature*, *297*, 43–47, doi:10.1038/297043a0.

Kurz, M. D., J. Curtice, D. Fornari, D. Geist, and M. Moreira (2009), Primitive neon from the center of the Galapagos hotspot, *Earth Planet. Sci. Lett.*, *286*, 23–34, doi:10.1016/j.epsl.2009.06.008.

Langmuir, C., et al. (1997), Hydrothermal vents near a mantle hot spot: the Lucky Strike vent field at 37°N on the Mid-Atlantic Ridge, *Earth Planet. Sci. Lett.*, *148*, 69–91, doi:10.1016/S0012-821X(97)00027-7.

Madureira, P., M. Moreira, J. Mata, and C. J. Allègre (2005), Primitive helium and neon isotopes in Terceira island (Azores archipelago), *Earth Planet. Sci. Lett.*, *233*, 429–440, doi:10.1016/j.epsl.2005.02.030.

Moreira, M., and C. J. Allègre (1998), Helium - Neon systematics and the structure of the mantle, *Chem. Geol.*, *147*, 53–59, doi:10.1016/S0009-2541(97)00171-X.

Moreira, M., and C. J. Allègre (2002), Rare gas systematics on Mid Atlantic Ridge (37° – 40°), *Earth Planet. Sci. Lett.*, *198*, 401–416, doi:10.1016/S0012-821X(02)00519-8.

Moreira, M., T. Staudacher, P. Sarda, J.-G. Schilling, and C. J. Allègre (1995), A primitive plume neon component in MORB: The Shona ridge-anomaly, South Atlantic (51 – 52°S), *Earth Planet. Sci. Lett.*, *133*, 367–377, doi:10.1016/0012-821X(95)00080-V.

Moreira, M., J. Kunz, and C. J. Allègre (1998), Rare gas systematics on popping rock: Estimates of isotopic and elemental compositions in the upper mantle, *Science*, *279*, 1178–1181, doi:10.1126/science.279.5354.1178.

Moreira, M., R. Doucelance, B. Dupré, M. Kurz, and C. J. Allègre (1999), Helium and lead isotope geochemistry in the Azores archipelago, *Earth Planet. Sci. Lett.*, *169*, 189–205, doi:10.1016/S0012-821X(99)00071-0.

Moreira, M., K. Breddam, J. Curtice, and M. Kurz (2001), Solar neon in the Icelandic mantle: Evidence for an undegassed lower mantle, *Earth Planet. Sci. Lett.*, *185*, 15–23, doi:10.1016/S0012-821X(00)00351-4.

Poreda, R., J. G. Schilling, and H. Craig (1986), Helium and hydrogen isotopes in ocean-ridge basalts north and south of Iceland, *Earth Planet. Sci. Lett.*, *78*, 1–17, doi:10.1016/0012-821X(86)90168-8.

Raquin, A., and M. Moreira (2009), Air $^{38}\text{Ar}/^{36}\text{Ar}$ in the mantle: Implication on the nature of the parent bodies of the Earth, *Earth Planet. Sci. Lett.*, *287*, 551–558, doi:10.1016/j.epsl.2009.09.003.

Sarda, P., T. Staudacher, and C. J. Allègre (1988), Neon isotopes in submarine basalts, *Earth Planet. Sci. Lett.*, *91*, 73–88, doi:10.1016/0012-821X(88)90152-5.

Sarda, P., M. Moreira, T. Staudacher, J.-G. Schilling, and C. J. Allègre (2000), Rare gas systematics on the southernmost Mid-Atlantic Ridge: Constraints on the lower mantle and the Dupal source, *J. Geophys. Res.*, *105*, 5973–5996, doi:10.1029/1999JB900282.

Singh, S. C., W. Crawford, H. Carton, T. Seher, V. Combier, M. Cannat, J. P. Canales, D. Dusunur, J. Escartin, and J. M. Miranda (2006), Discovery of a magma chamber and faults beneath a Mid-Atlantic Ridge hydrothermal field, *Nature*, *442*, 1029–1032, doi:10.1038/nature05105.

Staudacher, T., P. Sarda, S. H. Richardson, C. J. Allègre, I. Sagna, and L. V. Dmitriev (1989), Noble gases in basalt glasses from a Mid-Atlantic ridge topographic high at 14°N : Geodynamic consequences, *Earth Planet. Sci. Lett.*, *96*, 119–133, doi:10.1016/0012-821X(89)90127-1.

Stroncik, N. A., S. Niedermann, and K. Haase (2008), Plume-ridge interaction revisited: Evidence for melt mixing from He, Ne and Ar isotope and abundance systematics, *Earth Planet. Sci. Lett.*, *268*, 424–432, doi:10.1016/j.epsl.2008.01.037.

Stuart, F. M., S. Lass-Evans, J. G. Fitton, and R. M. Ellam (2003), High $^3\text{He}/^4\text{He}$ ratios in picritic basalts from Baffin Island and the role of a mixed reservoir in mantle plumes, *Nature*, *424*, 57–59, doi:10.1038/nature01711.

- Trieloff, M., J. Kunz, D. A. Clague, D. Harrison, and C. J. Allègre (2000), The nature of pristine noble gases in mantle plumes, *Science*, 288, 1036–1038, doi:10.1126/science.288.5468.1036.
- Valbracht, P. J., T. Staudacher, A. Malahoff, and C. J. Allègre (1997), Noble gas systematics of deep rift zone glasses from Loihi seamount, Hawaii, *Earth Planet. Sci. Lett.*, 150, 399–411, doi:10.1016/S0012-821X(97)00094-0.
- Yang, T., Y. Shen, S. van der Lee, S. C. Solomon, and H. Shu-Hue (2006), Upper mantle structure beneath the Azores hotspot from finite-frequency seismic tomography, *Earth Planet. Sci. Lett.*, 250, 11–26, doi:10.1016/j.epsl.2006.07.031.
- Yokochi, R., and B. Marty (2004), A determination of the neon isotopic composition of the deep mantle, *Earth Planet. Sci. Lett.*, 225, 77–88, doi:10.1016/j.epsl.2004.06.010.
-
- A. Bezos, Laboratoire de Planetologie et de Géodynamique de Nantes, Faculté des Sciences, 2 rue de la Houssinière, BP 92208, F-44322 Nantes, CEDEX 3, France.
- M. Cannat, J. Escartin, E. Gayer, F. Guillon, C. Hamelin, and M. Moreira, Institut de Physique du Globe de Paris, Sorbonne Paris Cité CNRS, UMR 7154, 1 rue Jussieu, F-75238 Paris, CEDEX, France. (moreira@ipgp.fr)